NONLINEAR SOIL-STRUCTURE INTERACTION DUE TO BASE SLAB UPLIFT ON THE SEISMIC RESPONSE OF AN HTGR PLANT

R.P. KENNEDY, S.A. SHORT
Holmes & Narver, Inc., Anaheim, California 92801, U.S.A.

D.A. WESLEY, T.H. LEE
General Atomic Company, San Diego, California 92138, U.S.A.

SUMMARY

Two major reasons have been expressed as to why dynamic base slab uplift should be minimized: (1) As nuclear power plants are normally designed for seismic loadings based upon linear analysis, and since soil-structure interaction becomes nonlinear when only a portion of the base slab is in contact with the soil, linear elastic analysis may be unacceptable if base slab uplift occurs (as the resultant design loads may be incorrect), and (2) substantial uplift could cause excessive toe pressures in the supporting soil and significant impact forces when the slab recontacts the soil. The primary purpose of this paper was to evaluate the importance of the nonlinear soil-structure interaction effects resulting from substantial base slab uplift occurring during a seismic excitation. That is, will there be either significant shifts in magnitude or frequency of structural response or excessive toe pressures and large heel uplift distances when there is significant base slab uplift.

The structure considered for this investigation consisted of the containment building and prestressed concrete reactor vessel (PCRV) for a typical HTGR plant. A simplified dynamic mathematical model was utilized consisting of a conventional lumped mass structure with soil-structure interaction accounted for by translational and rotational springs whose properties are determined by elastic half space theory. Three different site soil conditions (a rock site, a moderately stiff soil and a soft soil site) and two levels of horizontal ground motion (0.3 g and 0.5 g earthquakes) were considered.

Based upon the parametric cases analyzed in this investigation, it may be concluded that linear analysis (which ignores the nonlinear soil-structure interaction effects of base slab uplift) can be used to conservatively estimate the important behavior of the base slab, even under conditions of substantial base slab uplift. For all cases investigated here, linear analysis resulted in higher base overturning moments, greater toe pressures, and greater heel uplift distances than nonlinear analyses.

It may also be concluded that the nonlinear effect of uplift does not result in any significant lengthening of the fundamental period of the structure. Also, except in the short period region (period less than half of the fundamental period) only negligible differences exist between in-structure response spectra based on linear analysis and those based on nonlinear analysis.

Finally, it can be concluded that for sites in which soil-structure interaction is not significant, as for the rock site, the peak structural response (shears and moments) at all locations above the base mat are not significantly influenced by the nonlinear effects of base slab uplift. However, for the two soil sites, the peak shears and moments are, in a few instances, significantly different between linear and nonlinear analyses.

As a result, linear analysis may be used to determine all structural response for rock sites even when there is substantial base slab uplift. However, for soil sites, nonlinear analyses are necessary if substantial base slab uplift occurs.

1. INTRODUCTION

In high seismic regions it has often been the practice to use oversized base slabs for the major nuclear power plant structures in order to prevent or at least minimize the amount of dynamic base slab uplift which will result from the overturning moments developed during seismic ground motion. Two major reasons have been expressed as to why dynamic base slab uplift should be minimized:

1. Nuclear power plant structures and equipment therein are normally designed based upon the results of linear elastic dynamic analyses to incorporate the effect of earthquake loadings. If a portion of the base slab uplifts, then the stiffness effect of the soil-structure interface will be reduced since only a portion of the base slab remains in contact with the soil. This stiffness reduction can change the frequency content and dynamic response calculated for the structure. Thus, linear elastic analyses may be unacceptable as the resultant loads used to design structures and equipment may be incorrect if base slab uplift occurs.
2. If substantial uplift were allowed this would increase the pressures on the supporting soil at the toe-end of the base slab and the heel-end of the slab would lift off of the supporting soil. Excessive toe pressures could result. If the heel-end were to lift off a substantial amount, this could result in significant impact forces being generated when the heel-end recontacts the soil.

It is of interest to determine whether substantial base slab uplift from the supporting soil results in either significant shifts in the magnitude or frequency of structural response or in excessive toe pressures or large heel uplift distances. If neither condition occurs, then dynamic base slab uplift does not need to be prevented or minimized.

For three different soil conditions (ranging from a soft soil site to a stiff rock site) this paper investigates the consequences of base slab uplift which result because of the inability of the base slab-soil interface to support tensile stresses. For each soil condition, both linear and nonlinear dynamic analyses (accounting for nonlinear soil-structure interaction resulting from base slab uplift) were performed on the containment building and prestressed concrete reactor vessel (PCRV) for a typical High Temperature Gas Cooled Reactor (HTGR) Plant. For the results presented here, a very simplified dynamic mathematical model of a typical HTGR containment building and PCRV complex was utilized, and the earthquake time-history was applied in only a single horizontal direction. The mathematical model of the reinforced concrete reactor containment building and the PCRV on a common base slab as utilized for this paper is illustrated in Figure 1. An artificial earthquake time-history whose response spectrum envelopes the horizontal design spectra given in U.S. AEC Regulatory Guide 1.60 [1] was utilized. Analyses were performed for peak ground accelerations of both 0.3g's and 0.5g's. Soil-structure interaction was modeled using equivalent horizontal translational and rocking soil springs which were given nonlinear properties to account for the effect of uplift. The three different soil site conditions considered are defined as: Site A - Rock Site, shear wave velocity = 5900 fps; Site B - Moderately Stiff Soil Site, shear wave velocity = 1900 fps; and Site C - Soft Soil Site, shear wave velocity = 1076 fps.

In addition, this paper presents a simple, very efficient approach to incorporate localized nonlinearities (such as soil-structure interaction) into a linear elastic analysis

such that this form of nonlinear analysis is nearly as efficient as a linear elastic time-history analysis.

2. NONLINEAR SOIL-STRUCTURE INTERACTION

2.1 LINEAR ELASTIC BASE SPRING PROPERTIES

When the structure moves relative to the surrounding soil mass, resisting forces are developed not only along the bottom of the base slab but also along the side walls. Figure 2 shows the resisting forces applied at the soil-structure interface and the equivalent soil springs utilized. The base translational spring stiffness K_{T_B} is developed from the soil compliances associated with the base shear force V_B located at the bottom of the base slab. The base rotational spring K_{R_B} is developed from the soil compliances associated with the base moment M_B resulting from rocking type normal forces spread over the entire rectangular plan area of the base slab. The side horizontal translational spring K_{T_S} located a distance i (Figure 2) above the bottom of the base slab and rotational spring K_{R_S} are included to account for the stiffening influence of the normal force P_S and moment M_S resulting from distributed normal pressure applied to the side walls of the penetration building, and base slab. Side spring stiffness values were computed in accordance with procedures recommended in Reference [2].

The elastic base spring properties K_{T_B} and K_{R_B} are calculated based upon the formulas proposed by Whitman and Richart (1967) and contained in Reference [3] which are only strictly applicable for the condition of a rigid base slab resting on the surface of an elastic half-space.

For the rectangular base the translational and rocking base stiffnesses are:

$$K_{T_B} = 2(1+\nu)\, G\beta_x \sqrt{WL} \qquad \text{eq. (1)}$$

$$K_{R_B} = \frac{G}{1-\nu}\, \beta_\psi\, WL^2 \qquad \text{eq. (2)}$$

where G and ν are soil material properties, W and L are the width and length of the base slab, β_x, and β_ψ are defined in Reference [3]. So long as L/W is between 0.5 and 2.0, the factors β_x and β_ψ can be considered to be essentially constant.

2.2 NONLINEAR ELASTIC SOIL-STRUCTURE INTERACTION MODEL

With sufficient overturning moment there is a tendency for a portion of the base slab to lift off the underlying supporting rock because the soil-structure interface does not have the capacity to transmit tension. Figure 3 illustrates the behavior of the base slab under the assumption that no uplift tension can develop at the soil-slab interface. At the bottom of the slab the soil-slab interface is subjected to a vertical load P_B, an overturning moment M_B, and a lateral shear V_B. The overturning moment M_B and lateral shear V_B shown in this figure are the values associated with the soil springs K_{R_B} and K_{T_B} and represent the moment and shear which must be transmitted to the soil through the bottom of the base slab. It is assumed that the interface pressure varies linearly across the length of the slab. Based upon this assumption, uplift will result when:

$$\left|M_B\right| \geq M_U = \frac{P_B L}{6} \qquad \text{eq. (3)}$$

Prior to uplift initiation ($M_B \leq M_U$), the entire slab is in contact (D=L); the base stiffnesses K_{T_B} and K_{R_B} are given by Equations (1) and (2); and the toe pressure by:

$$P_t = \frac{P_B}{LW} + \frac{6M_B}{L^2W} \qquad (|M_B| \leq M_U) \qquad \text{eq. (4)}$$

Assuming no interface tensile capacity, once the base moment M_B exceeds the uplift moment M_U only a portion of the base slab remains in contact; the toe pressures rise; and the base spring stiffnesses soften. The amount of slab in contact is given by:

$$D/L = 1.5 - \frac{M_B}{2M_U} \qquad (|M_B| \geq M_U) \qquad \text{eq. (5)}$$

while toe pressure is given by:

$$P_t = \frac{2P_B}{DW} \qquad (|M_B| \geq M_U) \qquad \text{eq. (6)}$$

The heel uplift δ_h is given by:

$$\delta_h = L\left(1 - \frac{D}{L}\right)\theta \qquad \text{eq. (7)}$$

2.2.1 Nonlinear Base Moment - Rotational Relationship

As the slab uplifts, the base rotational stiffness softens because less slab remains in contact with the underlying rock. As shown in Equation (2), the rocking stiffness is proportional to the square of the length of slab D which remains in contact with the supporting soil as long as $\beta\psi$ remains approximately constant. Several reasonable approaches are available to obtain base-moment-rotational relationships for uplifted slabs. Probably the most rigorous approach would be to perform a series of static three-dimensional nonlinear no-tension finite element analyses of the base slab-supporting soil elastic half-space system for the combination of vertical axial load P_B and a wide range of overturning moments M_B. From the results of a series of such analyses it would be possible to develop a nonlinear moment-rotation relationship for conditions in which only a portion D of the slab is in contact. Two simpler approaches appear also to be reasonable. One is to assume that for a slab contact length D, the secant base rotational stiffness $K_{R_{BS}}$ can be approximated by substituting the contact length D into the rotational stiffness equation (Equation (2)). In this case, one would obtain as an approximation [4] that:

$$K_{R_{BS}} = K_{R_B}\left(\frac{D}{L}\right)^2 = \frac{K_{R_B}}{\alpha}\left[3 + \frac{2}{\alpha}\left(1 - \sqrt{3\alpha + 1}\right)\right] \qquad \text{eq. (8)}$$

where K_{R_B} is the initial linear rotational base stiffness as given by Equation (2) and

$$\alpha = \frac{|\theta|}{\theta_U} \quad \text{for } |\theta| > \theta_U \text{ and } \alpha = 1 \text{ for } |\theta| \leq \theta_U \; ; \; \theta_U = \frac{M_U}{K_{R_B}}$$

in which θ is the base rotation associated with the base moment M_B, M_U is the moment at which uplift is initiated (as given by Equation (3)), and θ_U is the rotation at which uplift is initiated. Another possible assumption is to assume that the nonlinear tangent rota-

tional stiffness $K_{R_{BT}}$ can be directly approximated by substituting the contact length D into Equation (2). The moment-rotation relationship for each assumption are shown in Figure 4. The nonlinear moment-rotation relationship based upon the secant assumption predicts a greater amount of nonlinear behavior than that based upon the tangent assumption. Since the primary purpose of this paper is to compare results obtained from linear and nonlinear analyses for base slab uplift it was decided to use the secant assumption so as to possibly overemphasize the degree of nonlinearity involved.

2.2.2 Nonlinear Base Translational Stiffness

As the base uplifts due to base rotation θ the translational base stiffness is also reduced below its linear elastic value K_{T_B} because less of the slab is in contact. Similarly, as for rotational stiffness, the nonlinear base translational secant stiffness $K_{T_{BS}}$ can be related to the linear base translational stiffness K_{T_B} by:

$$K_{T_{BS}} = K_{T_B} \left[D/L\right]^{1/2} = K_{T_B} \left[1.5 - \frac{\left|M_B\right|}{2M_U}\right]^{1/2} \qquad \text{eq. (9)}$$

2.2.3 Determination of Effective Vertical Load on the Base Slab

It is necessary to determine the moment M_U at which uplift is initiated. This uplift moment M_U is a function of the effective vertical base load P_B which at any time t is approximately given by:

$$P_{B_t} = P_{DL} \left(1 + a_{v_t}\right) - B \qquad \text{eq. (10)}$$

where P_{DL} is the total structure weight, a_{v_t} is the vertical ground acceleration at time t, and B is the uplift buoyancy due to a portion of the structure being below the water table. Since a_{v_t} varies with time, P_{B_t} also actually varies with time and thus, the uplift moment M_U and rotation θ_U vary with time. This means that to be rigorous, one would have to apply independent vertical and horizontal acceleration time-histories concurrently to perform a nonlinear dynamic analysis. However, to obtain the maximum difference between the linear and nonlinear results, the minimum value of P_{B_t} was utilized as determined by substituting the negative value of $a_{v_{max}}$ into Equation (10). For all analyses a maximum vertical acceleration $a_{v_{max}}$ equal to 0.24g's was used.

3. METHOD OF NONLINEAR ANALYSIS USED

With completely generalized nonlinear behavior, one would normally perform the time-history analysis using a numerical step-by-step integration method without taking advantage of modal decoupling because, under conditions of generalized nonlinear behavior, mode shapes and modal frequencies have no meaning. However, when the nonlinear behavior is very localized, such as in this case where only the base soil spring behaves nonlinearly, one can perform the nonlinear time-history analysis using modal superposition after determining linear elastic mode shapes and modal frequencies. Basically, the method consists of dividing the nonlinear stiffness matrix up into two components; a linear stiffness matrix based upon the initial stiffnesses, and nonlinear correction stiffness terms. The nonlinear correction stiffness terms can then be replaced through the usage of properly applied equivalent nonlinear correction forces (to correct for the fact that the system is not linear) the magnitude of which are determined at each time step. These nonlinear correction forces can then be treated similarly to all other externally applied dynamic forces or

accelerations. Thus, the analysis can be converted into an equivalent linear analysis (for which modal analysis is applicable) to which nonlinear correction forces are applied at each time step.

Usage of this method has many advantages for cases with only a few localized nonlinearities. First, the computational time to perform nonlinear time-history analysis for a very localized nonlinearity is only negligibly longer than the time required for linear analysis. Secondly, since there is generally a far less number of significant modes than the total number of degrees of freedom, the computational effort and time is greatly reduced by decoupling the equations of equilibrium through modal analysis. Third, an "exact" time-history integration routine can be used for the time step analyses of each mode since the modal frequency is known. Usage of an "exact" integration routine eliminates problems of numerical stability and the possible introduction of artificial damping. This enables greater accuracy to be obtained while marching the analysis at relatively long time step increments.

3.1 NONLINEAR CORRECTION FORCES

The nonlinear base spring has initial translational and rotational stiffnesses of K_{T_B} and K_{R_B}, respectively. However, as the base rotation θ_B increases, these springs soften and for a given value of θ_B the secant translational and rotational stiffnesses are $K_{T_{BS}}$ and $K_{R_{BS}}$, respectively. The base shear and moment reactions applied to the base node at any time can be written in terms of the initial stiffnesses and correction forces:

$$V_B = K_{T_{BS}}(\delta_B) = K_{T_B}\delta_B - P_{BC}$$
$$M_B = K_{R_{BS}}(\theta_B) = K_{R_B}\theta_B - M_{BC} \qquad \text{eq. (11)}$$

where δ_B is the base translation and P_{BC} and M_{BC} are a nonlinear correction force and moment applied at the base node and are given by:

$$P_{BC} = K_{T_B}\delta_B\left[1 - \left(K_{T_{BS}}/K_{T_B}\right)\right]$$
$$M_{BC} = K_{R_B}\theta_B\left[1 - \left(K_{R_{BS}}/K_{R_B}\right)\right] \qquad \text{eq. (12)}$$

where $K_{T_{BS}}/K_{T_B}$, and $K_{R_{BS}}/K_{R_B}$, are functions of the ratio of base rotation θ_B to the rotation θ_U at which uplift is initiated. Thus, the nonlinear base spring forces and moments can be completely defined in terms of equivalent linear stiffnesses K_{T_B} and K_{R_B} and correction forces P_{BC} and M_{BC}.

3.2 ANALYTICAL PROCEDURE

The dynamic equation of equilibrium for applied horizontal ground acceleration, a_x and correction forces P_{BC} and M_{BC} applied to the base node is:

$$[M]\{\ddot{x}\} + [C]\{\dot{x}\} + [K_s]\{x\} = -\begin{Bmatrix} m_x \\ 0 \end{Bmatrix} a_x + \begin{Bmatrix} P_{BC} \\ 0 \\ M_{BC} \\ 0 \end{Bmatrix} \qquad \text{eq. (13)}$$

in which $\{\ddot{x}\}$, $\{\dot{x}\}$ and $\{x\}$ are column vectors of relative translational and rotational accelerations, velocities and displacements, $[K_s]$ is the equivalent linear stiffness matrix

for the overall system, and the correction force vector only contains a force and moment term applied of the base node. In development of the linear structure stiffness matrix the base spring stiffnesses are taken as the linear stiffnesses K_{T_B} and K_{R_B} (based upon the initial stiffness). All nonlinear effects are accounted for by the application of correction forces P_{BC} and M_{BC}.

The basic method of dynamic analysis used is the mode superposition method in which the undamped modal frequencies ω_m and their corresponding mode shapes $\{\phi\}_m$ are used to decouple the equation of dynamic equilibrium into M modal equations of the form:

$$\ddot{Z}_m + 2\,\omega_m\lambda_m\,\dot{Z}_m + \omega_m^2\,Z_m = P_m^{**} \qquad \text{eq. (14)}$$

where P_m^{**} represents the m-th modal force as expressed by

$$P_m^{**} = \{\phi\}_m^T \{P^*\} \qquad \text{eq. (15)}$$

where P* is the load vector on the righthand side of Equation (13) or:

$$\{P^*\} = -\begin{Bmatrix} m_x \\ 0 \end{Bmatrix} a_x + \begin{Bmatrix} P_{BC} \\ 0 \\ M_{BC} \\ 0 \end{Bmatrix} \qquad \text{eq. (16)}$$

The nodal displacements $\{X\}$ can then be expressed in terms of the modal displacements $\{Z\}$.

Equation (14) represents the dynamic equation of equilibrium for mode m. For each mode of interest, the solution is obtained by breaking the time-history up into a number of equally spaced time points. Knowing the modal acceleration, velocity and displacement at time t_i and the variation of P_m^{**} during the time step from t_i to t_{i+1}, one can determine the modal acceleration, velocity, and displacement at time t_{i+1}. The modal force P_m^{**} associated with mode m is a function of both the ground acceleration a_x and the nonlinear correction forces P_{BC} and M_{BC} applied at the base node. The ground acceleration a_x is specified at each time step. The correction forces P_{BC} and M_{BC} are a function of the nodal displacement and rotation of the base node and as such are known at time t_i and all previous times but are unknown at time t_{i+1}. The value of P_{BC} and M_{BC} to be used during the time step from t_i to t_{i+1} are obtained by linear extrapolation of their value from time t_{i-1} and t_i.

The solution technique employed for the solution of the uncoupled equations of motion was a modified version of the Nigam and Jennings [5] method. This solution technique involves the use of the exact modal acceleration-time-history variation between any two time increments in lieu of an assumed variation and the usage of explicit integration of this time-history in lieu of numerical integration. With this technique, accurate nonlinear solutions were obtained with a time step of 0.005 seconds.

4. COMPARISON OF LINEAR AND NONLINEAR RESPONSE ANALYSES

4.1 BASE SLAB RESPONSE

The maximum base slab linear and nonlinear responses for each of the cases considered is compared in Table I. In the linear analyses the initial linear soil-structure interaction stiffnesses are used throughout the analyses. In the nonlinear analyses the nonlinear soil-structure interaction stiffnesses defined previously are used whenever the base slab is in a state of uplift. The maximum base overturning moment M_B and

maximum base rotation θ are determined from these analyses. The ratio D/L, heel uplift δh, and toe pressure P_t for both the linear and nonlinear analyses are determined from M_B and θ based upon Equations (5), (6) and (7) which assume no interface tensile capacity. Comparisons between the linear and nonlinear results shows that nonlinear analyses predict lower base overturning moments and higher base rotations than predicted by linear analyses. For all the cases considered, the nonlinear analyses predict that a significant portion of the base slab remains in contact even when the linear analysis predicts that nearly the entire slab will uplift. Thus, the portion of a slab which might uplift is never as great as one would predict based upon linear analysis. The largest predicted uplift of one inch, as given by linear analysis, occurs on the soft soil site (Site C). Considering that the base slab has a total length of 190 feet and is more than 16 feet thick, this height of uplift occurring at one end of the slab is considered to be negligible. Linear analyses always predict greater maximum toe pressures than nonlinear analyses. With the possible exception of uplift height (which is generally negligible) linear analysis conservatively overpredicts the response of the base slab.

Figure 5 presents a graph of D/L versus time for the nonlinear analysis of Sites A and C. Note that there are over 30 instances of uplift for the approximately 10 seconds of strong ground motion but that only about 15 of these instances are significant in magnitude. Also note that the duration of each uplift is very short and that the total duration that the slab is in a state of uplift is also very short compared to the duration of the strong ground motion. It can be concluded that uplift is a very short transient phenomenon and does not significantly effect the base slab.

4.2 VARIATION OF PEAK STRUCTURAL RESPONSE WITH HEIGHT

Figures 6 and 7 present comparisons of linear and nonlinear analyses results versus height for the containment building and PCRV for peak accelerations and moments, respectively. Even for the 0.5g earthquake in which 88 percent (based on linear analysis) of the base slab uplifts, Site A shows only small differences between linear and nonlinear analyses. Peak accelerations differed by less than 20 percent while peak moments differed by less than 10 percent at all locations. Peak displacements (not shown) differ negligibly between linear and nonlinear analyses while sheears differ similarly as the differences in moments. The peak responses of the containment building and the PCRV are only slightly influenced by base slab uplift on the rock site. For the soil sites (Sites B and C) greater differences between the peak linear and nonlinear responses do occur in a few instances. It is somewhat difficult to make general statements on these differences. What is apparent, however, is the fact that the nonlinear effects can be more significant for soil sites.

4.3 COMPARISON OF IN-STRUCTURE (FLOOR) RESPONSE SPECTRA

In-Structure (Floor) Response Spectra have been developed and compared for the linear and nonlinear time-history results for various locations on the containment building and the PCRV. Figures 8, 9, and 10 present comparisons of the in-structure spectra from linear and nonlinear analyses generated at the top of the PCRV. For Site A (Rock Site) even with the 0.5g earthquake in which linear analysis predicts that 88 percent of the base slab uplifts essentially no difference exists between spectra predicted from linear and nonlinear analyses except in the low period region (below 0.05 second period). The nonlinear behavior due to

base slab uplift does not cause a significant shift in the frequency of peak spectral response. In the low period range, the response spectra from the nonlinear analysis tends to be higher than those from linear analysis. Each time the base uplifts and then closes to recontact the underlying soil, some slapdown forces are generated upon closure. These forces excite a higher coupled structure translational and base rotational mode of response which for Site A has a natural period of 0.02 second. For the soil sites (Sites B and C) the nonlinear effects of base slab uplift tend to have a significant influence upon the in-structure response spectra generated. The softening of the soil-structure interaction stiffnesses does not appear to significantly lengthen the period of the first mode of response of the structure; probably because the base slab is in a state of uplift only for very short durations of time. However, the nonlinear soil-structure interaction due to base slab uplift excites higher modes of response substantially more than is predicted by assuming linear soil-structure interaction in which base slab uplift is ignored. Thus, in the low period region the in-structure response spectra generated from a nonlinear analysis are substantially greater than those generated from a linear analysis.

4.4 ACCURACY OF NONLINEAR ANALYSES

A method for performing nonlinear analysis for base slab uplift which is only negligibly more expensive than linear analysis has been outlined in Section 3 and used for the results reported. Separate analyses were carried out to provide an independent verification of the nonlinear analysis results determined by using this correction force method. These verifying analyses were made by solving the coupled nonlinear governing equations through direct integration using a standard integration scheme known as the Gill's version of Runge-Kutta process and a time step of 0.0002 second. The numerical results of the base slab responses generated by using direct integration are also shown in Table I compared with the corresponding values obtained by the nonlinear correction force method. The nonlinear in-structure response spectra at the PCRV top head for Site C are compared in Figure 10. It is apparent that the two different approaches exhibit excellent agreement.

5. CONCLUSIONS

Even under conditions of substantial base slab uplift, linear analysis (which ignores the nonlinear soil-structure interaction effects of base slab uplift) can be used to conservatively estimate the important behavior of the base slab. Calculated peak base overturning moments are greater when based upon linear analysis than when based upon nonlinear uplift analyses. Since linear analysis leads to greater calculated overturning moments, it follows that linear analysis will predict a greater portion of the slab has uplifted than would be predicted based upon a nonlinear analysis. In fact, the differences can be substantial particularly when linear analysis has predicted that a significant portion of the slab uplifts. Toe pressure calculated based upon the overturning moment from a linear analysis appears to always be greater (often much greater) than that based upon nonlinear analysis. The height of base slab uplift appears to remain negligibly small (one inch or less) even under conditions of very soft soil with 70 percent of the base slab uplifted.

On a rock site, linear analysis in which the effect of base slab uplift is ignored provides good results for peak structural responses and in-structure response

spectra as long as the linear analysis does not predict that more than 50 percent of the base slab has uplifted. When more than 50 percent of the base slab is predicted to uplift, it may be necessary to perform a nonlinear analysis accounting for the influence of uplift to adequately predict the in-structure response spectra in the short period region. On soil sites the influence of soil-structure interaction even without uplift may be very significant on the response. When soil-structure interaction is very significant, then it appears to be necessary to perform nonlinear analyses incorporating the effect of base slab uplift in order to accurately determine the in-structure response spectra and peak structural responses whenever linear analysis predicts more than one-third of the base slab uplifts.

So long as the influence of uplift is accounted for in the generation of in-structure response spectra and the determination of peak structural responses and so long as the calculated toe pressures are not excessive, there does not appear to be any necessity to prevent base slab uplift.

This paper represents the summarization and extension of work originally performed [4] under contract to the Electric Power Development Company of Japan.

6. REFERENCES

[1] "Design Response Spectra for Seismic Design of Nuclear Power Plants," Regulatory Guide 1.60, Directorate of Regulatory Standards, United States Atomic Energy Commission, October 1973.

[2] Akino, K., and H. Tajimi, "A Seismic Design and Dynamic Analysis of Nuclear Power Plants," Nuclear Structural Engineering, Vol. 1, 1965, Part 1, pp 232-238; Part 2, pp. 120-125.

[3] Richart, F. E., J. R. Hall, and R. D. Woods, Vibrations of Soils and Foundations, Prentice-Hall, Englewood Cliffs, New Jersey, 1970.

[4] Kennedy, R. P., S. A. Short, R. E. Bachman, and A. W. Chow, "Seismic Analysis of Containment Building and Prestressed Concrete Reactor Vessel Complex for EPDC High Temperature Gas-Cooled Reactor (HTGR)," prepared for General Atomic Company, NSS-8196.1, Holmes & Narver, Inc., Anaheim, Calif., June 1974.

[5] Nigam, N. C., and P. C. Jennings, "Digital Calculation of Response Spectra from Strong-Motion Earthquake Records," Earthquake Engineering Research Laboratory, California Institute of Technology, Pasadena, Calif., 1968.

TABLE I

COMPARISON OF BASE SLAB RESPONSES FOR LINEAR AND NONLINEAR ANALYSES

Parameter	Site A 0.3g		Site A 0.5g		Site B 0.3g		Site C 0.3g	
	Linear	Nonlinear	Linear	Nonlinear	Linear	Nonlinear	Linear	Nonlinear
Maximum Base Overturning Moment M_B (kip-ft)	10.40×10^6	9.81×10^6 (9.78×10^6)	17.33×10^6	13.43×10^6 (13.39×10^6)	14.27×10^6	10.19×10^6 (10.13×10^6)	15.11×10^6	9.84×10^6 (9.78×10^6)
Maximum Base Rotation θ (radians)	1.000×10^{-5}	1.835×10^{-5} (1.817×10^{-5})	1.666×10^{-5}	7.108×10^{-5} (6.886×10^{-5})	18.010×10^{-5}	27.19×10^{-5} (26.45×10^{-5})	63.43×10^{-5}	80.60×10^{-5} (79.20×10^{-5})
Slab Contact Ratio D/L	.671	.718 (.721)	.118	.429 (.432)	.362	.687 (.692)	.295	.715 (.721)
Heel Liftoff Height δ_h (inches)	.008	.012	.034	.093	.262	.194	1.021	.524
Toe Pressure P_T (kips per square foot)	14.1	13.2	80.2	22.1	26.2	13.8	32.1	13.2

Values in parentheses are results obtained by direct nonlinear integration for comparison with results from nonlinear correction force technique.

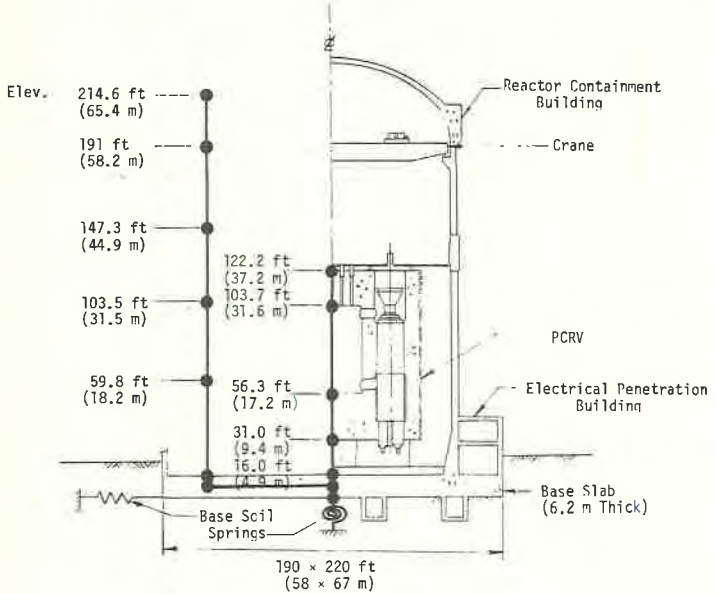

FIGURE 1

HTGR CONTAINMENT BUILDING, PCRV AND PENETRATION BUILDING WITH MATHEMATICAL MODEL USED

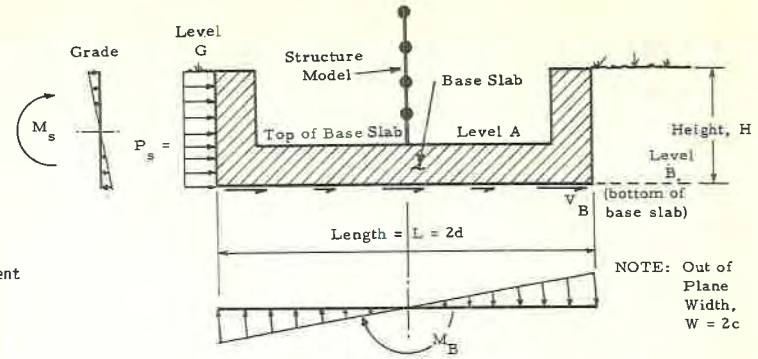

a. Soil Resistance Forces

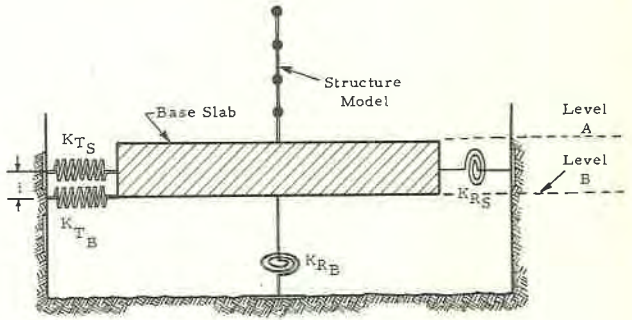

b. Equivalent Soil Springs

FIGURE 2

EQUIVALENT SOIL-SPRING MODEL OF SOIL STIFFNESS

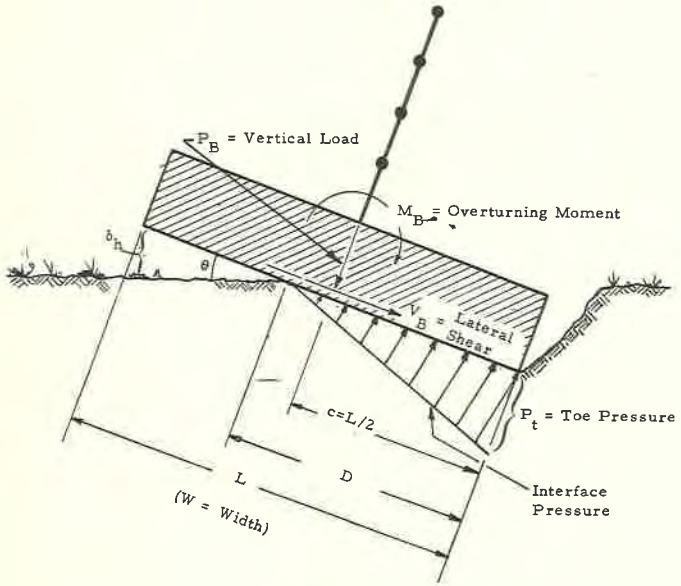

FIGURE 3

BASE SLAB ROCKING SHOWING UPLIFT

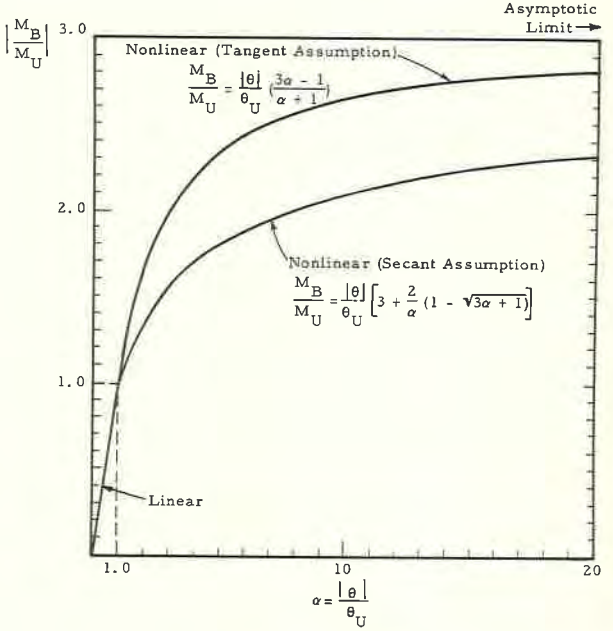

FIGURE 4

NONLINEAR BASE MOMENT-ROTATION RELATIONSHIP

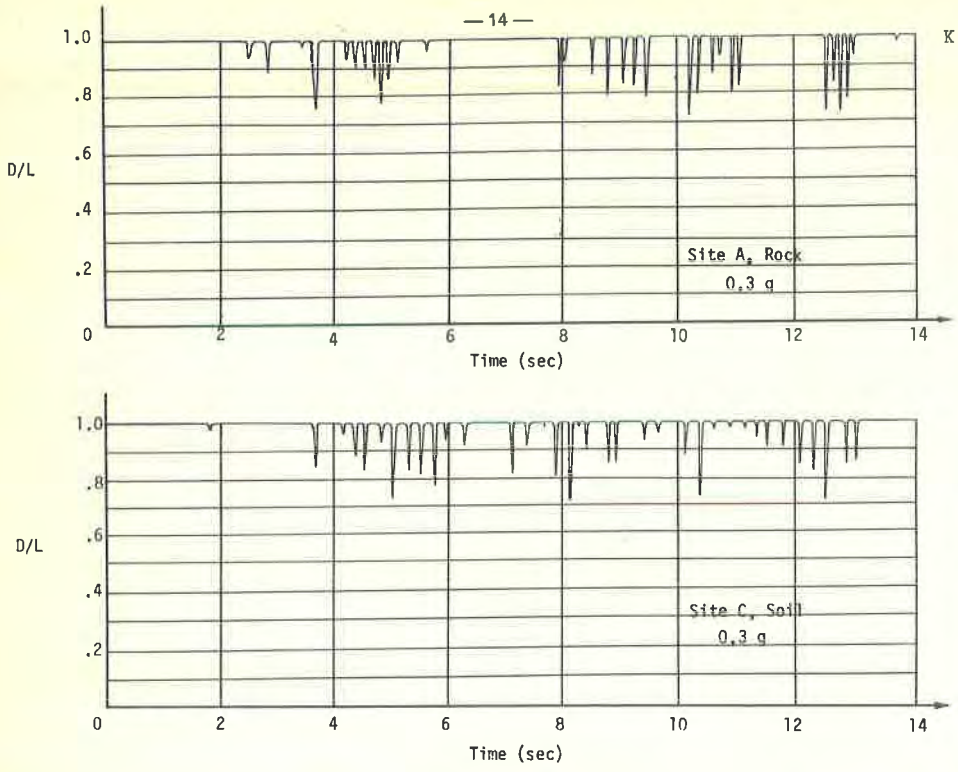

FIGURE 5

VARIATION OF D/L PARAMETER AS FUNCTION OF TIME

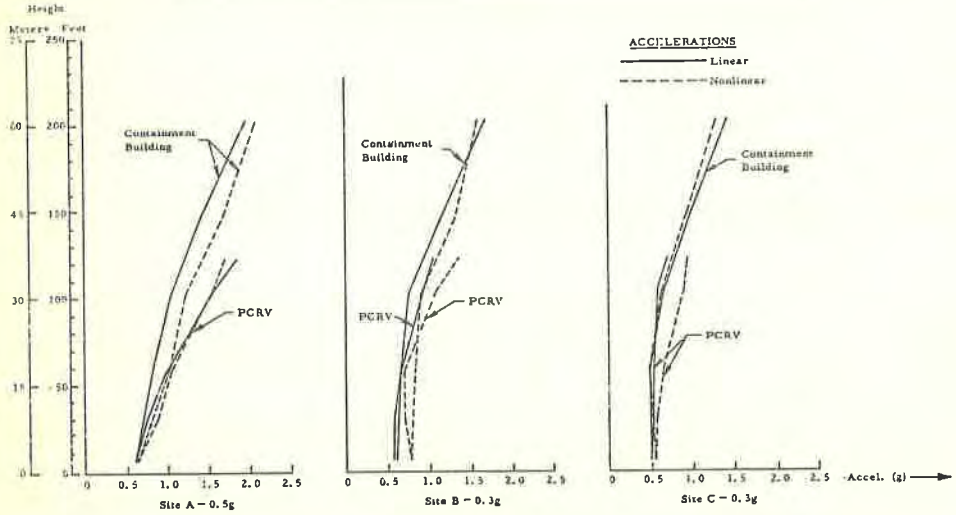

FIGURE 6

COMPARISON OF LINEAR AND NONLINEAR STRUCTURAL RESPONSE OF CONTAINMENT BUILDING AND PCRV - ACCELERATIONS

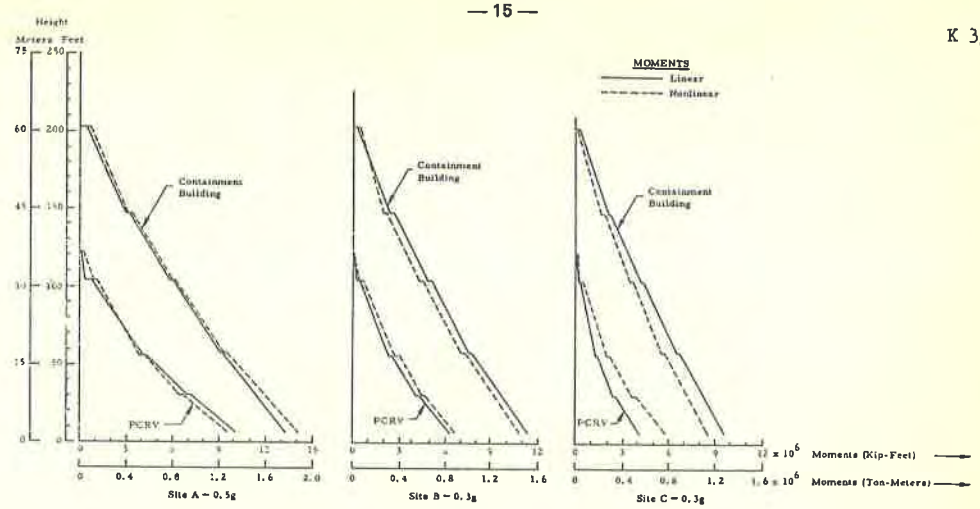

FIGURE 7

COMPARISON OF LINEAR AND NONLINEAR STRUCTURAL RESPONSE OF CONTAINMENT BUILDING AND PCRV - MOMENTS

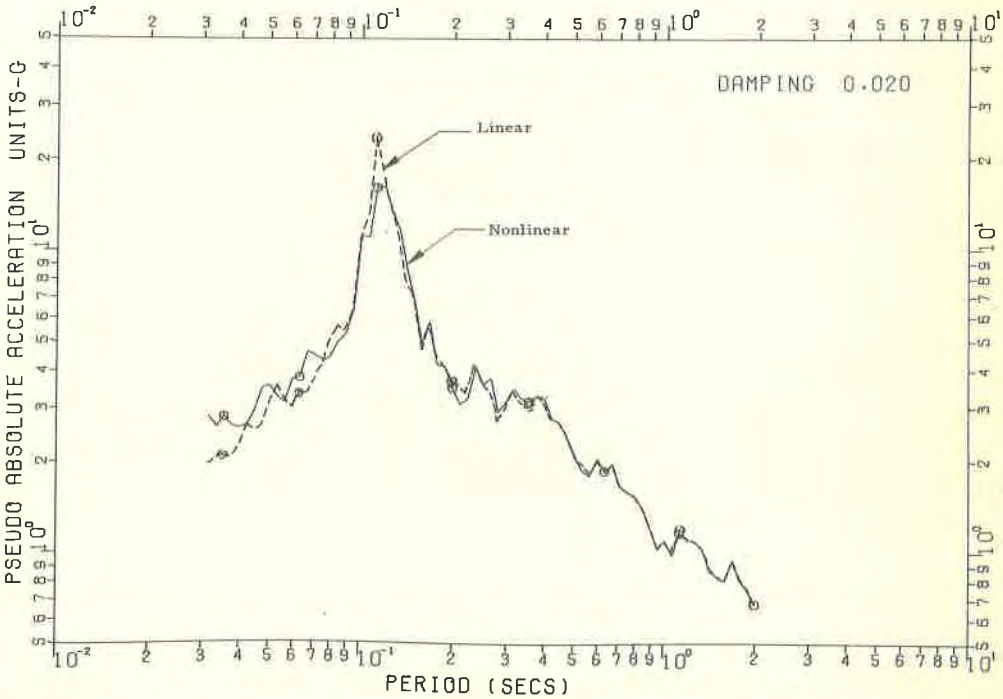

FIGURE 8

COMPUTED IN-STRUCTURE RESPONSE SPECTRA - TOP OF PCRV, SITE A, 0.5G

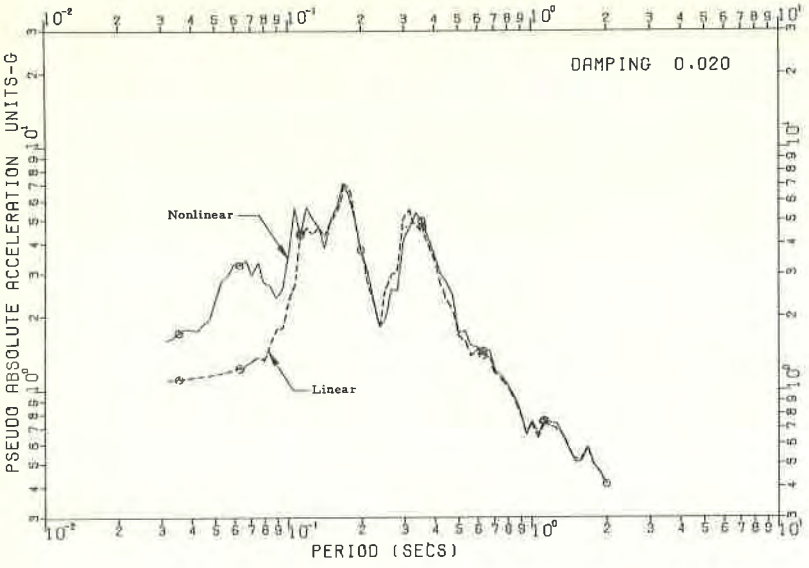

FIGURE 9

COMPUTED IN-STRUCTURE RESPONSE
SPECTRA - TOP OF PCRV, SITE B, 0.3G

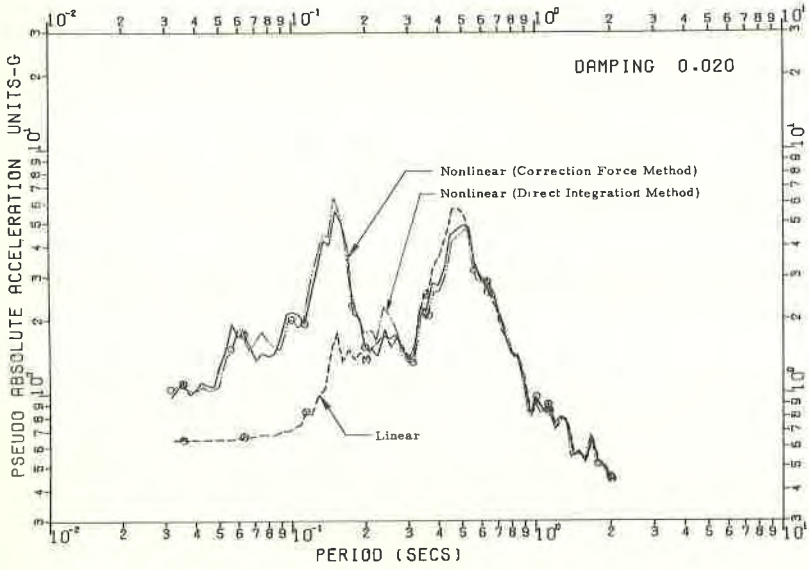

FIGURE 10

COMPUTED IN-STRUCTURE RESPONSE
SPECTRA - TOP OF PCRV, SITE C, 0.3G